JOURNAL OF NEUROPHYSIOLOGY
Vol. 76, No. 6, December 1996. Printed in U.S.A.

Neural Encoding of Shape: Responses of Cutaneous Mechanoreceptors to a Wavy Surface Stroked Across the Monkey Fingerpad

ROBERT H. LAMOTTE AND MANDAYAM A. SRINIVASAN
Department of Anesthesiology and Section of Neurobiology, Yale University School of Medicine, New Haven, Connecticut 06510; and Research Laboratory of Electronics and Department of Mechanical Engineering, Massachusetts Institute of Technology, Cambridge, Massachusetts 02139

SUMMARY AND CONCLUSIONS

1. The role of cutaneous mechanoreceptors in the tactile perception of shape was investigated. Objects whose surfaces were shaped as a pattern of smooth, alternating convex and concave cylindrical surfaces of differing radii of curvature were constructed such that there were no discontinuities in the slope of the surface. These "wavy surfaces" were stroked across the fingerpad of the anesthetized monkey and electrophysiological responses of slowly adapting type I mechanoreceptive afferents (SAs) and rapidly adapting type I mechanoreceptive afferents (RAs) were recorded.

2. For both SAs and RAs, each convexity indenting the skin evoked a burst of impulses and each concavity of the same curvature that followed elicited a pause in response. "Spatial event plots" (SEPs) of the occurrence of action potentials as a function of the location of the object on the receptive field were obtained and interpreted as the responses of a spatially distributed population of fibers. With increasing magnitude of curvature (equivalently, decreasing radius of curvature) of convexity, the mean width of the burst in the SEPs for each fiber type (representing the width of a region of skin containing active fibers) decreased and the mean discharge rate during the burst increased. Over a range of velocities of stroking from 1 to 40 mm/s, the number of RAs activated increased with velocity, whereas SAs were active at all velocities. For both SAs and RAs, the burst rates increased with velocity, whereas the widths of the bursts and pauses remained approximately invariant. Thus the spatial measures of burst or pause width provide a robust representation of the size of a feature on the object surface.

3. For a given velocity of stroking, the spatially distributed pattern of averaged discharge rates (spatial rate profile, SRP) provided a representation of the shape of the wavy surface. The distance between neighboring peaks in the SRP for individual RAs and SAs was approximately the same as the distance between the peaks of the wavy surface. The averaged SRP for a population of SAs provided a better representation of shape than that for RAs. Whereas active regions in the SEP can be isomorphic to the two dimensional form of the stimulus "footprint" in contact with the skin surface, the SRP, which in addition encodes the features of the stimulus in the third dimension normal to the skin surface, is not isomorphic to the stimulus shape.

4. When the sizes as well as the shapes of objects are varied, it is hypothesized that a central processing mechanism extracts the invariant property of shape from the slopes of the rising and falling phases of an SRP that has been normalized for overall differences in discharge rates. These differences would be expected to occur with variations in the parameters of stimulation such as compressional force, stroke trajectory, and stroke velocity. It was shown that a common feature of the mean SRP for SAs evoked by each wavy surface convexity, regardless of its radius, was the constancy of the slope from the base to the peak and from the peak to the base. Thus a possible code for the constant curvature of a cylinder is the constancy of the slopes along the rising and declining phases of the triangular-shaped spatial response profile evoked in the SA population by the cylindrical convexity.

INTRODUCTION

Tactile information about the shape of an object is provided through the activation of cutaneous mechanoreceptors. We will consider, for present purposes, the information obtained when touching an object with a single fingerpad, which contains the highest density of mechanoreceptors in the hand and has the highest spatial resolution (Darian-Smith and Kenins 1980; Johansson and Vallbo 1979; Johnson and Phillips 1981). Because the skin is pliable relative to a rigid object, it can conform to portions of the shape of an object that are of the appropriate height, area, and spacing and thereby receive a profile of indentation that is directly related to the contacting shape. The width of the region of contact is on the order of ≤ 1 cm for the human. The spatially distributed pattern of stresses and strains that activate the receptors located beneath the surface of the skin is a function not only of the shape of the object but also of the conditions of application of the object such as the contact force vector, velocity, and direction of translation and, finally, the mechânical filtering properties of skin. The resultant pattern of impulses generated in the active primary afferent fiber population contains, then, a wealth of information about the contact with the object from which the part that is directly related to shape must be extracted by a central processing mechanism.

The definition of an object's shape that is probably the most relevant to the corresponding neural representation is the distribution of curvatures on its surface (Srinivasan and LaMotte 1991). From differential geometry, it can be shown that the local curvature at each point on an object's surface, expressed as a function of distance along the surface, uniquely defines the object's shape (Gauss 1827). The local curvature is the reciprocal of the radius of a circle that can be fitted at a point on a given cross-sectional surface profile of the object. This definition is relevant to the neural encoding of shape for two reasons. First, unlike descriptions of shape that depend on an external system of coordinates, a distribution of curvatures is an intrinsic property of the object that remains the same for different translations and rotations of the object. Second, cutaneous mechanoreceptors are particularly sensitive to the edges (Johansson et al. 1982; Phillips and Johnson 1981; Vierck 1979) or, more generally speaking, regions of high curvature (LaMotte and Srinivasan

1987a; Srinivasan and LaMotte 1987). The spatial distribution of pressures exerted by an object against the skin is such that regions of maximum pressure occur where the changes in curvature and/or depths of indentation are high. For example, when a cylindrical bar indents the skin, modeled as a linear elastic half space, the maximum pressure varies inversely with the square root of the radius. Consequently, higher curvatures of the cylinder produce higher stresses and strains at receptor sites beneath the object even when the net contact force is the same (Srinivasan and LaMotte 1991).

Relatively small shapes, such as those with sizes of one or two contact regions on the fingerpad, can be discriminated solely on the basis of tactile cues alone (e.g., Goodwin et al. 1991; LaMotte and Srinivasan 1987a). That is, kinesthetic cues that might be available as the finger is stroked over a curved surface (e.g., Gordon and Morison 1982) are not required. Furthermore, when spherical shapes are passively indented into the fingerpad, humans are able to scale the perceived magnitude of curvature and the force of indentation independently (Goodwin and Wheat 1992). It is likely that the peripheral neural events contributing to the judgments of the curvature of objects pressed against but not stroked across the skin are provided primarily by he responses of slowly adapting (type I, Merkel cell) mechanoreceptive peripheral nerve fibers (SAs) and not by rapidly adapting Meissner corpuscle fibers (RAs) or pacinian corpuscle fibers (Srinivasan and LaMotte 1987). For example, SAs and not RAs respond to differences in the curvature of single cylindrical bars (LaMotte and Srinivasan 1993) and spheres (Goodwin et al. 1995) indented vertically into the monkey fingerpad.

In earlier studies, we also found that humans were able to discriminate, with the use of cutaneous cues alone, small differences in half-sinusoid step shapes that varied in wavelength from gradual to steep (LaMotte and Srinivasan 1987a,b; Srinivasan and LaMotte 1987). Each shape had a contour that changed smoothly from a flat surface on the low side of the step through a concave and then convex cylindrical curvature followed in turn by another flat surface on the high side. The shape was either statically pressed against or stroked across the fingerpad under maintained compressional force. Peripheral nerve fiber recordings in monkey were obtained with the use of these stimuli. It was found that the discharge rates of SAs were directly related to both the rate and magnitude of change in skin curvature. The discharge rates of RAs were modulated primarily by the rate of change in skin curvature but not the magnitude. It was concluded that for either stroking or vertical indentation, the spatial profile of responses in the SA population provided the best information on which the perceptual recognition of the shape as a sinusoidal step would be based. However, the smallest differences in curvature or step shape were best discriminated on the basis of differences in discharge rates of RAs during stroking and of SAs during vertical indentation.

The surfaces of most objects that typically come in contact with the fingerpad consist of multiple convexities and concavities of differing curvature and separation (wavelength). The purpose of the present study was to investigate the peripheral neural representation of such shapes. Specifically, the stimulus objects had a wavy surface with a smooth pattern of alternating convex and concave cylindrical surfaces of differing curvature. Portions of the results obtained have been summarized previously (LaMotte et al. 1993, 1994; Srinivasan and LaMotte 1991).

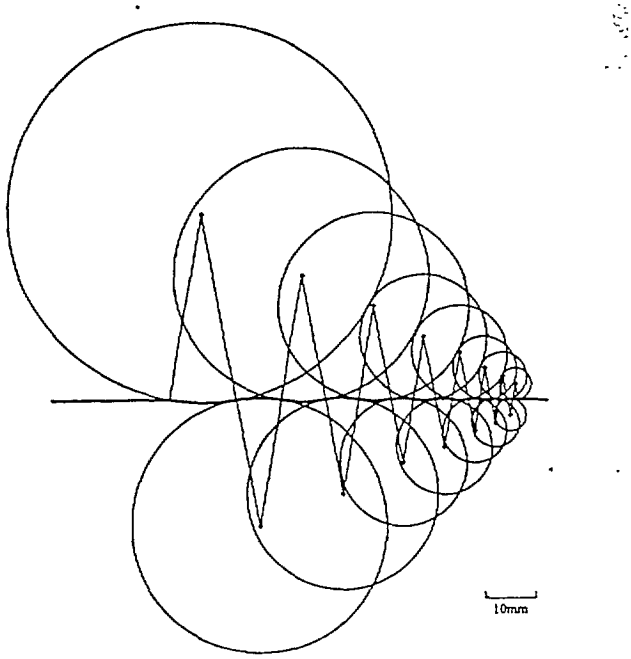

FIG. 1. Geometric procedure underlying the construction of the wavy surface. Convexities and concavities were arcs of circles. Each arc was fully defined by its radius of curvature and an angle of 20° subtended at the center (see METHODS). Bottom surface of the pattern was in contact with the fingerpad.

METHODS

Construction of curvature patterns

Two types of corrugated surfaces were used, each having a smooth pattern of alternating convex and concave cylindrical shapes designed so as to have a continuously changing surface slope. The convexities and concavities were arcs of circles, each arc fully defined by its radius of curvature and an angle of 20° subtended at its center. The dimensions were chosen such that each convexity and concavity was entirely in contact with the monkey finger during the experiments. Most experiments were carried out with the use of an aperiodic curvature pattern that had a succession of cylindrical curvatures (and radii) of 8 (1/8), 5.33 (3/16), 4 (1/4), 2.67 (3/8), 2 (1/2), 1.33 (3/4), 1 (1), and 0.67 (1.5) in.$^{-1}$ (Fig. 1). The corresponding curvatures (in m^{-1}) are 315, 210, 157, 105, 79, 52, 39, and 26. The second curvature pattern, used in only a few experiments, was periodic insofar as there were four cylindrical shapes for each curvature of 16, 8, and 5.33 in.$^{-1}$ and one cylinder of 4 in.$^{-1}$ (corresponding values in m^{-1} are 630, 315, 210, and 157). The aperiodic pattern was cut from aluminum, by means of a computer-controlled numerical milling machine, with a tolerance of 0.001 in. The periodic pattern was milled on the same machine from Plexiglas. The patterns used in the experiments were transparent epoxy replicas cast from rubber molds of the original specimens. Because each specimen was too long to be stroked in its entirety across the skin, each was divided into two parts. The pattern on the second part slightly overlapped that of the first. The responses of a mechanoreceptive fiber to each pattern could then be pieced together as though the entire pattern had been presented with a single stroke. None of the patterns had any perceptible fine surface texture.

Method of applying objects to the skin

The hand of the monkey was oriented with the palm up and maintained stationary by means of a screw glued to the fingernail and plasticine molded to the back of the hand. Once the fingerpad was oriented so that the center of the fiber's receptive field was facing upward toward the object, the screw was sunk into the plasticine and the plasticine was molded around the finger and the rest of the hand, but not along the sides of the fingerpad. This allowed the fingerpad to deform sideways in a natural way as the curvature pattern was stroked across the skin. The finger was typically angled upward by ~25° with respect to the horizontal plane.

In most of the experiments, the curvature pattern was applied by means of a stimulator with hydraulic actuators that were servo-controlled to provide precise control over position (2–10 μm) and velocity (±0.01 mm/s) in the vertical and horizontal axes, and over compressional force in the vertical axis (±3 to ±5 g wt) (LaMotte et al. 1982). The patterned surface was pressed against the fingerpad to achieve a desired force of 20 g wt. This force was then maintained (by small servo-controlled movements in the vertical axis) as the pattern was stroked across the finger at a velocity of 1, 5, 10, 20, or 40 mm/s. In most experiments a velocity of 10 mm/s was used. The stroking occurred in the horizontal plane and at right angles to the long axis of the finger.

In experiments with three fibers, the aperiodic curvature pattern was applied to the skin in the manner described except that another tactile stimulator was used that provided servo-control over compressional force at higher precision (less than ±0.5 g) by means of a high-speed torque motor (Cambridge Technology). The torque motor was mounted on a two-axis translation device (Anorad) that provided servo-control over position and velocity in the horizontal plane (LaMotte et al. 1993). No qualitative differences in results were obtained with the use of these two tactile stimulators.

Electrophysiological recordings

Evoked discharges in single mechanoreceptive peripheral nerve fibers were recorded extracellularly from small bundles of fibers microdissected from the upper median or ulnar nerve in the anesthetized monkey (LaMotte and Srinivasan 1987a). A total of 14 experiments was carried out in seven juvenile *Macaca fascicularis* monkeys. Recordings were obtained from 14 fibers. Seven were SAs and seven others were RAs classified as previously described (LaMotte and Srinivasan 1987a). Only fibers with receptive fields centrally located on the distal pads of the second, third, or fourth fingers were included in the study. The time of occurrence of each action potential, obtained from a voltage discriminator receiving input from a preamplifier, was recorded by means of an IBM PC computer and Lab Master (Axon Instruments). A general-purpose data collection computer program displayed the occurrence of each action potential and other digital events in real time on a video monitor, along with analog displays of compressional force and displacements of the curvature pattern along the vertical and horizontal axes.

Video recording

Von Frey-type monofilaments were used to map the border of the receptive fields under ×20 magnification with the use of a video camera mounted on a dissecting microscope. The finger was oriented so that the most sensitive spot (skin surface location having the lowest response threshold under monofilament stimulation) would lie directly beneath the curvature pattern. The ridges of the finger and a series of two to three roughly concentric receptive field maps (1 for each monofilament) were drawn on an acetate sheet mounted over the video screen showing the magnified view of the fingerpad. Several reference marks were drawn on the skin to aid in determining the location of the receptive field when stroking the pattern of curvatures across the skin. The horizontal location of the center of each convexity was marked with a thin line on the planar back side of the curvature pattern. The region of contact between the transparent stimulus pattern and the skin was video recorded. A video mixer added to the video recording the cumulative number of action potentials, compressional force, and elapsed time since the beginning of each trial, which included one stroke of the object across the skin.

When the video recording was played back in slow motion, the drawing of the receptive field (including papillary ridges and reference marks drawn on the skin) was aligned on the video screen with the video recorded image so that one could obtain the time elapsed from the beginning of a horizontal stroke for each reference mark on the curvature pattern to reach the most sensitive spot in the receptive field. This allowed us to take into account the lateral stretching of skin in aligning the temporal pattern of nerve impulses with the pattern of curvatures on the object. Because the velocity of stroking was known, the temporal occurrence of each action potential in response to the same object stroked in the two opposite directions could be plotted as a spatial location of the receptive field on the object.

Stimulus parameters

The two parts of the curvature pattern (see above) were each stroked back and forth over the fingerpad. At the beginning of a trial, the tactile stimulator moved the curvature pattern horizontally in the air above and at a right angle to the finger. The object was then brought vertically down onto the finger such that a region adjacent to the beginning of the first curvature indented the skin until the desired compressional force of 20 g was achieved. This force was then maintained as the object was stroked in the "forward" direction across the skin from one end of the pattern to the other end along a linear path oriented perpendicular to the long axis of the finger. The velocity of stroking was 1, 5, 10, 20, or 40 mm/s. The object was then withdrawn from the skin, thus ending the trial. The object remained in the same horizontal position until the next trial began 1 s later, at which time the object was indented into the skin and stroked at the same velocity in the "backward" direction (opposite to the forward), again maintaining a compressional force of 20 g. Typically, 12 strokes were delivered in each direction at each velocity, except for the velocity of 1 mm/s, at which only one stroke forward and one stroke backward were given.

RESULTS

General features of the responses of SAs and RAs to the curvature patterns

Responses to the aperiodic pattern stroked repeatedly in the same forward direction at 10 mm/s are shown for a typical SA in Fig. 2. The responsiveness of RAs to the same stimulus was more varied, as illustrated for two fibers in Fig. 3. A schematic of the wavy surface shows the eight raised portions (convexities) and the seven valleys in between (concavities). In these figures, at the start of a stroke, the monkey fingerpad was in contact with the flat portion on the left and the pattern was moved leftward, beginning stimulation with the lowest (broadest) curvature and ending with the highest. The overlapping traces in Fig. 2, *top*, show, respectively, the changes in the vertical position of the object and the compressional force of the object against the skin during each of 12 strokes. The ability of the tactile stimulator to maintain the force at the desired value of 20 g was better for higher than for lower curvatures. In experiments with

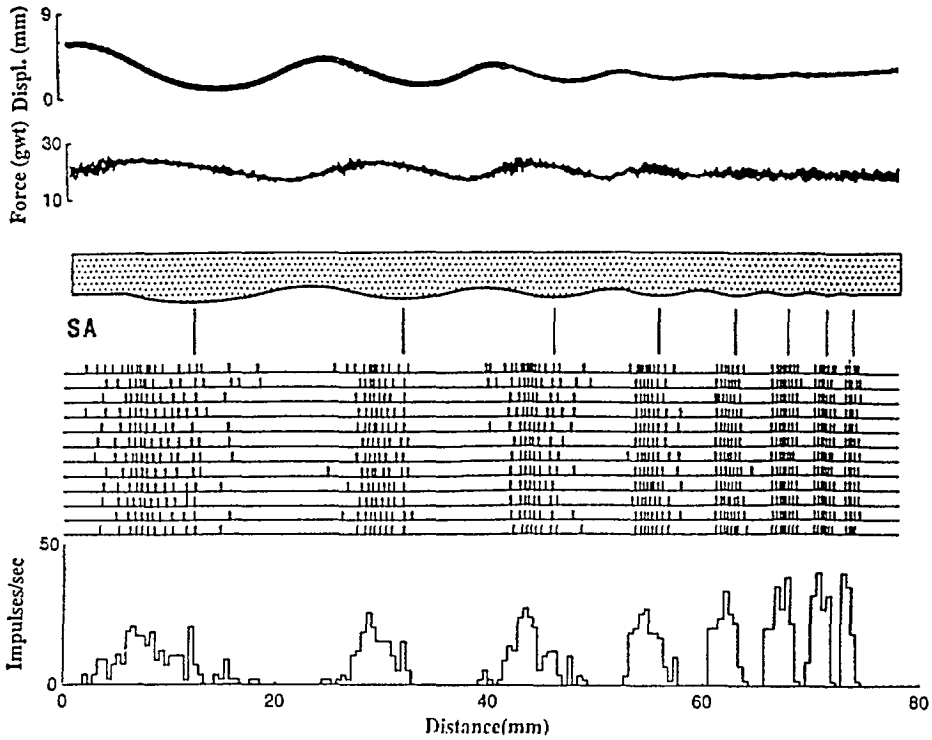

FIG. 2. Pattern of nerve impulses evoked in a slowly adapting mechanoreceptive fiber (SA) to the aperiodic pattern of curvatures stroked across the fingerpad. Temporal sequence of responses obtained in response to each stroke is plotted as a spatial profile (see text). Sequence of curvatures started with the lowest curvature, on the left side of the wavy surface, and ended with the highest, on the right. Vertical lines beneath the schematic of the aperiodic curvature pattern: location of the peak of each curvature. Vertical position of the object (Displ.) was changed under servocontrol to maintain the compressional force at ~20 g during stroking. Traces are superimposed for displacement and compressional force during a succession of 12 strokes at 10 mm/s in the same forward direction. Corresponding responses of the fiber to each stroke below are shown as vertical tick marks. Each mark is the location on the object of the most sensitive spot in the fiber's receptive field each time an action potential occurred. Histogram below impulse raster: mean discharge rate in imp/s calculated with the use of 0.5-mm bins.

some fibers the force control was considerably better than that shown in the figure, whereas in other experiments control was a little poorer, particularly for the lower curvatures. These minor differences in force control were sometimes responsible for changing the magnitude of response (total number of impulses) but not the overall pattern of response.

None of the fibers were spontaneously active, i.e., there was no ongoing discharge in the absence of a stimulus object. SAs and certain RAs responded with a burst of impulses when each convex portion of the wavy surface moved over the most sensitive spot in the receptive field. The nerve impulse rasters in Figs. 2–4 were each collected as a temporal sequence but are plotted as spatial event plots (SEPs) (Johnson and Hsaio 1992; Johnson and Lamb 1981). The object was stroked beginning with the flat surface next to the first broad convexity on the left and ending with the flat surface at the extreme right. Viewed as a temporal sequence, the origin of time for each stroke would be at the left, and the time scale is obtained by dividing the distance by the stroke velocity. There are two ways of viewing each pattern of impulses as a spatial sequence. First, one could imagine that the object was stationary and the skin of the fingerpad was moving over it at a velocity equal to the stroke velocity. Each vertical tick mark would represent the horizontal location of the center of the receptive field on the object's surface when a nerve impulse occurred as the fingerpad moved from left to right beneath the object. The second view, which is the one we will adopt, is to consider the impulse rasters as representing a snapshot of the instantaneous response of a hypothetical population of spatially distributed, continuous sheet of receptors with identical biomechanical and neural response properties. If the surface of the skin were considerably wider than the length of the wavy surface, then, at any instant of time during a stroke of the wavy surface, all the convexities would be in contact with the skin, and the nerve impulse tic marks could be viewed as the locations of the active receptors at that time. The widths of the bursts and pauses in response to convexities and concavities then represent regions of active and inactive receptor activity, respectively, with the discharge rate at each location representing the instantaneous frequency of discharge of the receptor at that location. However, in the present experiments, the skin of the fingerpad contacts the wavy surface at only one or a few of the convexities. Thus the variation of the population response over time is given by moving a window of width

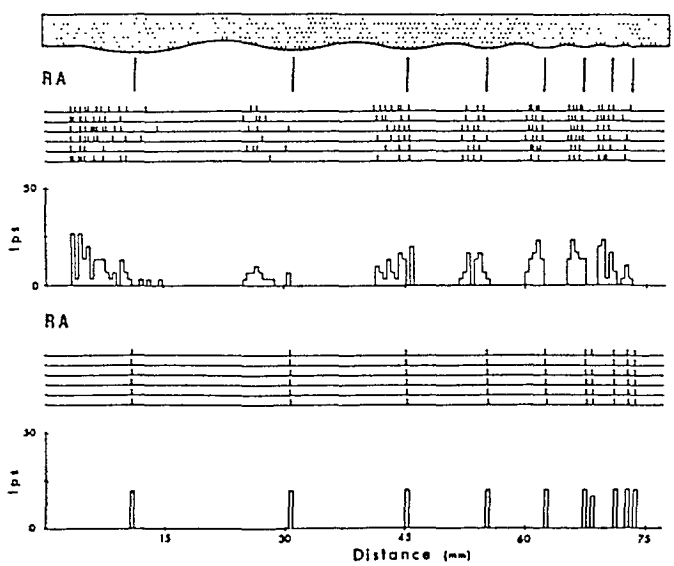

FIG. 3. Responses of 2 rapidly adapting mechanoreceptive fibers (RAs) to the aperiodic curvature pattern. Same format as Fig. 2. Discharge rate is given in imp/s (Ips).

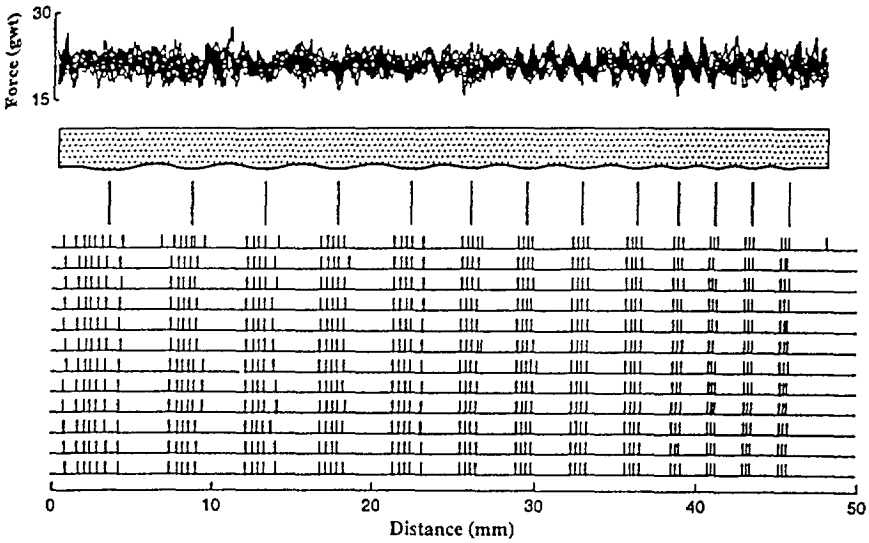

FIG. 4. Responses of an SA fiber to a periodic pattern of curvatures stroked across the fingerpad. There are 4 repetitions of each convex and concave curvature except for the unrepeated smallest 1 on the *left*. Note the regularity in the impulse patterns and in the total number of impulses for each stroke. Same format as in Fig. 2.

equal to the skin contact width from left to right (Figs. 2–4) with a velocity equal to the stroke velocity.

The spatial response profile (SRP), consisting of the discharge rate (averaged over all the strokes) plotted against the distance along the length of the wavy surface (e.g., histograms in Figs. 2, 3, and 6), was obtained for each fiber for strokes at 10 mm/s in the forward direction. The response rates of SAs and RAs were not isomorphically related to shape: the SRP consisted of triangular discharge rate profiles, one for each convexity. Also, each triangular profile was shifted toward the leading half of the convexity. The discharge rate correlated with the changes in the curvature of the skin produced by each shape. As a convexity moved over a fiber's receptive field, there was first a positively increasing change in curvature that evoked an increase in discharge rate. The discharge rate then decreased to zero as the curvature rate decreased to zero or became negative at the start of the following concavity. The peak discharge rate and the spatial gradient of the discharge rate evoked by each convexity increased as a function of increasing curvature. In the few cases where only one or two spikes were evoked by each convexity (e.g., Fig. 3, *bottom*), a precise capacity to encode the wavelength of the curvature pattern, by the sequence of interspike intervals, was still evident.

The pattern of discharge associated with each convexity was determined by that shape alone and not by the temporal pattern of preceding shapes. This is illustrated in Fig. 4 by the identical responses of an SA to each of four presentations of the same shape in the periodic pattern. The same result held for responses of another SA and an RA.

The major geometric features of these shapes were represented in the spatially distributed pattern of discharges, i.e., the shape of the discharge rate histogram evoked by each burst, the overall rate of discharge during the burst, and the widths of the burst and the pause between successive bursts. To measure the rates and widths of the responses to each shape, a vertical line was drawn on the SEP from top to bottom at the beginning and end of each burst of impulses. The location of each line was chosen, by eye, to include all of the impulses, grouped beneath a convexity, on ≥80% of the strokes. (If any impulses were excluded, they were clearly outliers and typically no more than 1 or 2). The "burst width" was defined as the distance (in mm) between the two lines drawn beneath a convexity and the discharge rate ("burst rate") was the number of impulses occurring between the lines divided by the duration of the burst. The mean burst rate corresponding to a given convexity was the average of the burst rates evoked on all the strokes (usually 12) delivered in the same direction. Measurements of burst width and rate were not made in the case where a single spike was evoked in response to a shape on most of the strokes (e.g., the RA response shown in Fig. 3, *bottom*). Repeated-measures analyses of variance were used to test the statistical significance of the main effects of, and interactions between, curvature, stroke velocity, stroke direction, and fiber type (SA vs. RA) on burst rate, burst width, and pause width.

Burst rate

The mean burst rate was modulated by changes in curvature for both SAs and RAs. The mean burst rate evoked by each convexity in the aperiodic pattern, stroked at 10 mm/s, was averaged for SAs and RAs separately for strokes in the forward and backward directions (Fig. 5). SAs and RAs exhibited the same increase of approximately threefold in burst rate over the range of curvatures tested. There was a significant effect of curvature on discharge rate for both SAs and RAs ($P < 0.001$) but no significant overall differences due to fiber type or the direction of stroking ($P > 0.1$).

The burst rate was not only modulated by changes in curvature but also by changes in stroke velocity (Fig. 6). Only forward strokes were delivered in this experiment. The burst rates of SAs and RAs each increased significantly with stroke velocity ($P < 0.006$) over the range of 1–40 mm/s. The increase was greater for higher than for lower curvatures. In contrast, both the impulse count per burst and the impulse count per millimeter decreased with stroke velocity. There was no overall difference in the burst rates between SAs and RAs ($P > 0.5$). Most RAs did not respond to the pattern at the slowest velocities of 1 and 5 mm/s (for which data are not plotted in the figure), whereas all did respond

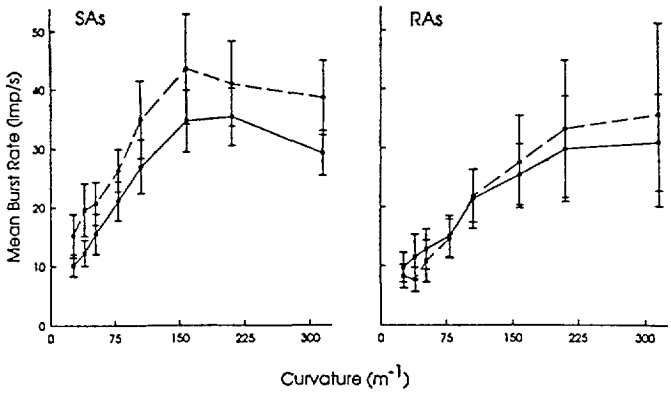

FIG. 5. Effect of convex curvature on the mean discharge rates ("burst rates") of SAs and RAs. Aperiodic pattern was stroked forward and backward (—— and — — —, respectively) at 10 mm/s. Each data point is the mean ± SE of the mean rate for 12 strokes obtained from each fiber (7 SAs and 7 RAs).

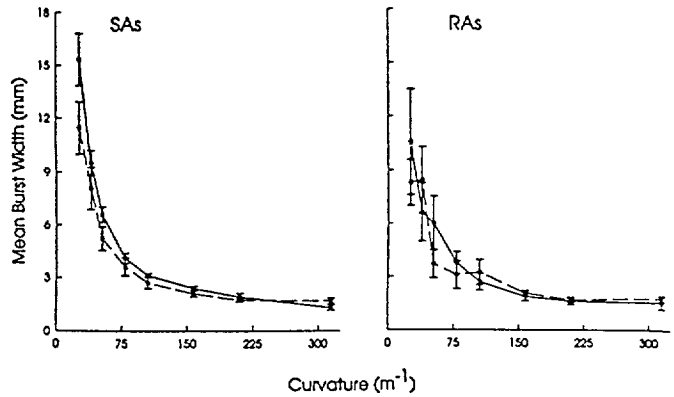

FIG. 7. Effect of convex curvature on the widths of the bursts evoked in SAs and RAs. Solid and dashed lines: forward and backward strokes, respectively. Stroke velocity: 10 mm/s. Each data point is the mean width of response over 12 strokes for 7 SAs and 7 RAs.

to stroke velocities of ≥10 mm/s. One RA responded to strokes at 10 mm/s with only one or two impulses per convexity (Fig. 3, *bottom*). Another responded with one or two impulses to the higher curvatures and failed to respond to the lower ones. In some experiments, we measured the threshold for the RA response to different velocities of vertical indentation with a cylindrical bar. Those RAs responding poorly to lateral stroke velocities of ≤10 mm/s had higher velocity thresholds to vertical indentation. Thus only SAs provided information about curvature when the object was stroked very slowly over the skin.

Widths of bursts and pauses

The mean widths of bursts (Fig. 7) and pauses (Fig. 8) evoked in SAs and in RAs by each curvature in the aperiodic pattern were obtained for strokes in each direction. There was a significant nonlinear decrease in the mean burst widths of SAs and of RAs with increasing curvature for either direction of stroking ($P < 0.001$). There were no significant differences between the burst widths of the two fiber types or the two directions of stroking ($P > 0.08$). The same held true for the widths of pauses between bursts. The pause widths decreased significantly with increasing curvature for both directions of stroking for each fiber type ($P < 0.001$). No significant differences were found between the pause widths of RAs and SAs ($P > 0.1$).

Both burst and pause width were found to increase linearly with increasing radius of the convexity and concavity and were approximately equal (within ~10% deviation) to the corresponding arc length.

The velocity of stroking had no significant effect ($P > 0.1$) on the widths of bursts of SAs and RAs (Fig. 9), in contrast to the strong effect that velocity had on burst rates (Fig. 6). Similarly, the widths of pauses between bursts changed insignificantly with changes in stroke velocity ($P > 0.1$) (Fig. 10). As stated in the case of burst rate, RAs provide less information, if any, than SAs about the widths of convexities or concavities in the curvature pattern at the slower stroke velocities of ≤5 mm/s.

Neuronal representation of spatial wavelength

In the SRP, the distance between the peak discharge rates (the "peak rate separation") evoked by adjacent convex portions of the wavy surface was taken as a neuronal representation of the physical distances separating the convexities. The peak rate separation was averaged for SAs and for RAs and plotted against the physical distance (wavelength) separating the adjacent peaks of convexities (Fig. 11). The mean peak rate separations for both SAs and RAs were linearly related and nearly identical to the physical wavelength.

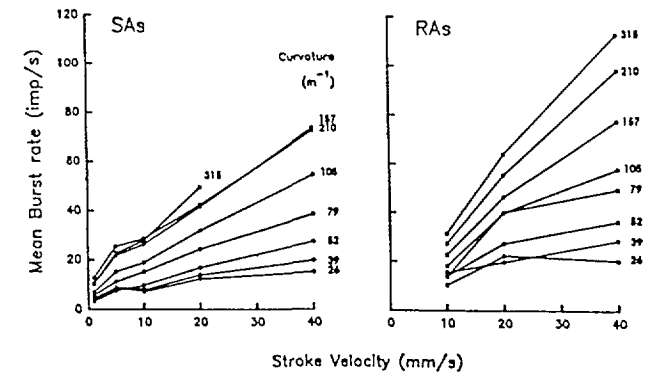

FIG. 6. Effect of stroke velocity on the burst rates evoked by convexities of different curvature. Each data point is the mean burst rate obtained from the mean responses to 12 strokes in the same (forward) direction in each of 3 fibers.

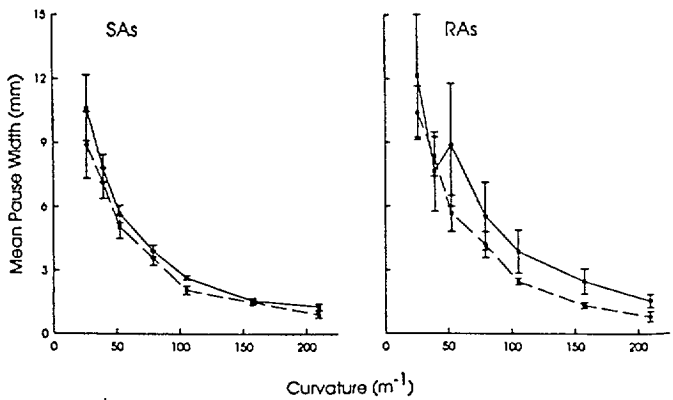

FIG. 8. Effects of concave curvature on widths of pauses between bursts. Same format as in Fig. 7.

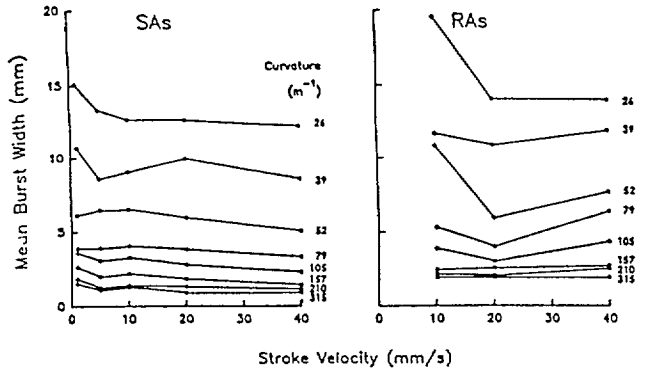

FIG. 9. Effects of different stroke velocities on the widths of the bursts evoked by convexities of different curvature. Each data point is the mean response of 3 SAs and 3 RAs over 12 strokes in the forward direction.

Those RAs that responded with only one or two impulses to each convexity encoded the distances separating convexities as well as if not better than those fibers responding with a greater number of impulses.

Shape of the spatially distributed discharge rates for the SA and RA populations

To investigate the relationship between the shapes in the aperiodic curvature pattern and the pattern of responses in a spatially distributed population of SAs and RAs, the average SRP among the fibers stimulated at a stroke velocity of 10mm/s was obtained for strokes in each direction. Then, a sliding average (3 bins or 1.5 mm) was used for smoothing the profile (Fig. 12). Note that although each convex-concave curvature pair evoked a burst followed by a pause in each fiber, when the responses in each SRP were averaged across fibers there was a slight blurring of the response pattern. This was due in small part to the choice of binwidth and the sliding average but primarily to the slight differences in the onset of each fiber's response to each convexity, which produced small shifts in the spatial location of each response when plotted against one curvature pattern.

For either direction of stroking, the SRP of the SAs to the different convexities was smoother than that of RAs and had a more consistent shape. For the RAs, there were sometimes two discharge peaks associated with each convexity (especially the 3 or 4 broadest curvatures). This property, as well as a greater responsiveness

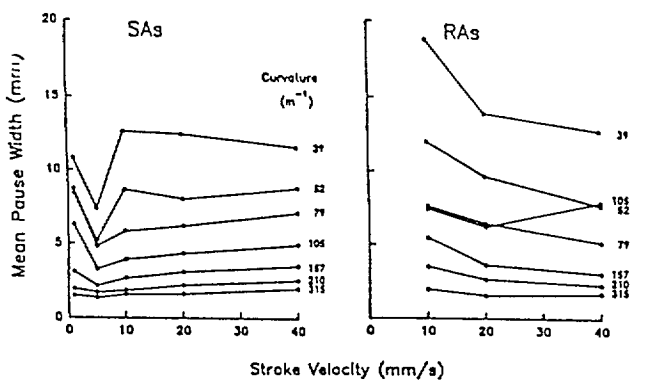

FIG. 10. Effects of different stroke velocities on the widths of the pauses between impulse bursts for concavities of different curvature. Same format as in Fig. 9.

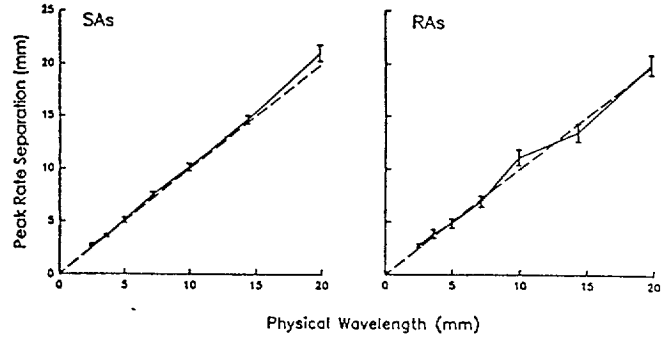

FIG. 11. Relationship between the mean distance separating adjacent peak discharge rates in the spatial response profiles of SAs and RAs and the corresponding physical separation between adjacent points of maximum convex curvature on the wavy surface (wavelength). The distances separating adjacent peak discharge rates in the spatial rate profiles obtained from each fiber for 12 strokes at 10 mm/s in the forward direction (e.g., Figs. 2 and 3) were averaged separately for SAs and for RAs. The average distance measures were then plotted against the corresponding physical distances separating the centers of adjacent convexities on the wavy surface. Dashed lines: equality of the 2 distance measures.

to small, transient vibrations produced by perturbations in force control, stick-slip of skin, etc., may have contributed to the irregularity in RA profiles in relation to those of SAs.

When the responses to the opposite directions of stroking are overlaid in Fig. 12, *bottom*, the peaks of discharge rates are located on either side of the centers of the broader convexities; the distance between the peaks grows smaller as a function of increasing curvature. The peak rate evoked by each convexity typically does not occur at the peak of each convexity. Its locus on the fingerpad will differ for each convexity and, for a given convexity, will differ for the two directions of stroking. The figure also suggests that the overall contrast in peak discharge rates between the largest and the smallest curvatures is greater for RAs than for SAs. This contrast would be expected to increase as stroke velocity is decreased to a value below the velocity thresholds of an increasing number of RAs.

The spatial profiles of discharge rates in response to different velocities of stroking were not computed because only three fibers of each type were tested and the number of impulses evoked at higher velocities was too small to provide a reliable shape of the profile.

To estimate the overall rate of change in the discharge rates of SAs associated with each convexity in the pattern, a straight line was fitted by eye to the rising and falling phases of each mound in the profile in Fig. 12, i.e., from trough to peak and vice versa. (This analysis was not practical to undertake for the RA data because of the irregular shapes of their SRP.) In the cases where there was a small "shoulder" near the bottom of the trough, e.g., first and second mounds from the left Fig. 12, *top left*, only the data above the shoulder were used. The absolute value of each slope is plotted separately in Fig. 13 for the rising and falling phases of the response to each convexity for each direction of stroking. The slopes were greater for the backward direction (Fig. 12, *middle*), largely because of the overall greater number of impulses evoked. This was due to the responses of a few fibers that were more responsive to backward than to forward strokes. The widths of the averaged bursts evoked by a given convexity were about the same for the two direc-

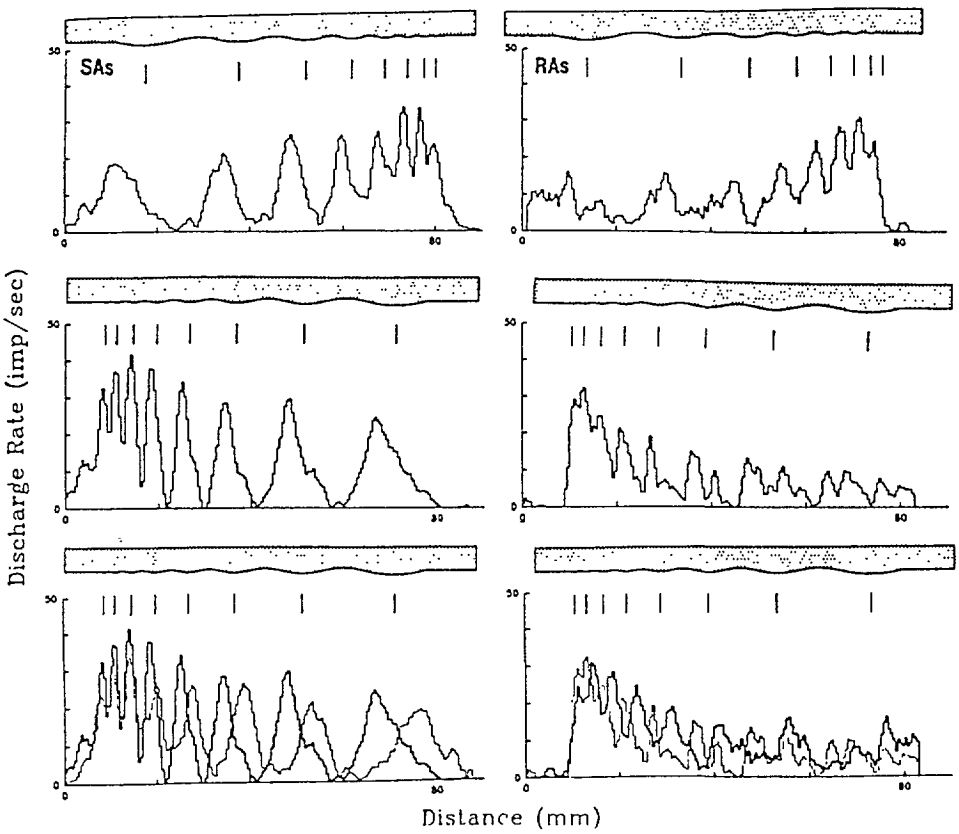

FIG. 12. Spatial profiles of mean discharge rates evoked in SAs and RAs. A sliding average across 3 bins was used. Curvature pattern was stroked at 10 mm/s in the forward and backward directions (*top* and *middle*, respectively). *Bottom*: responses to the 2 directions are superimposed (the profile for forward stroking is a mirror image of that in the *top*). Binwidth: 0.5 mm.

tions and, for a given direction, the slopes of the leading and trailing sides of the discharge profile evoked by a given convexity were about the same.

If the peak discharge rate associated with a shape stroked in the forward direction were normalized to that elicited by the same shape stroked backward, the slopes for the two directions should be about the same. This is suggested by the curves in Fig. 13, where the scale for each panel was chosen so that the highest slope was about the same distance from the horizontal axis of the graphs. Therefore the relative changes in the slope of the spatial profile of discharge rates in the SA population might pro-

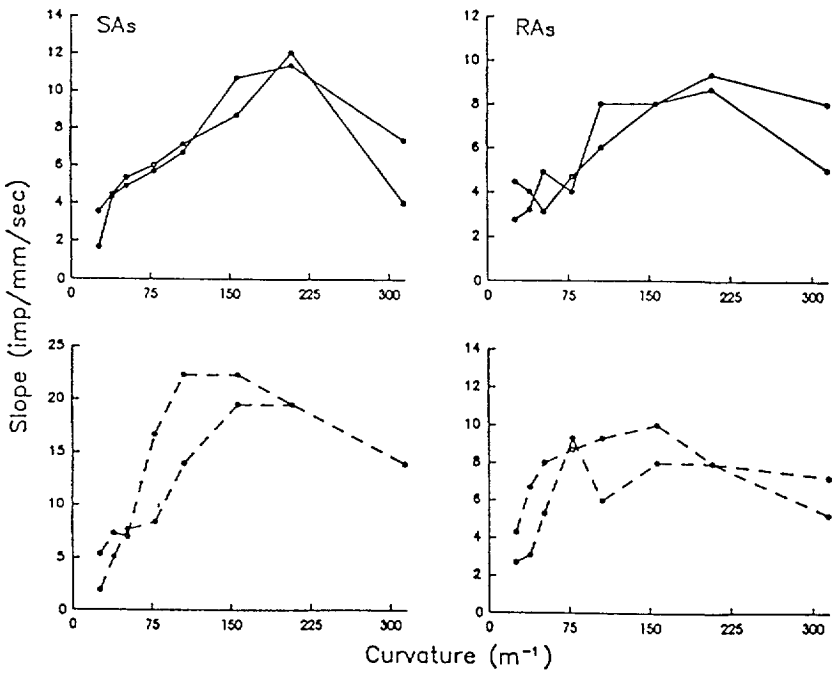

FIG. 13. Slopes of the rising and falling phases of the peak discharge rates of SAs evoked in response to each convexity. Open and filled circles: rising and falling phases, respectively, for forward (——) and backward (— — —) strokes.

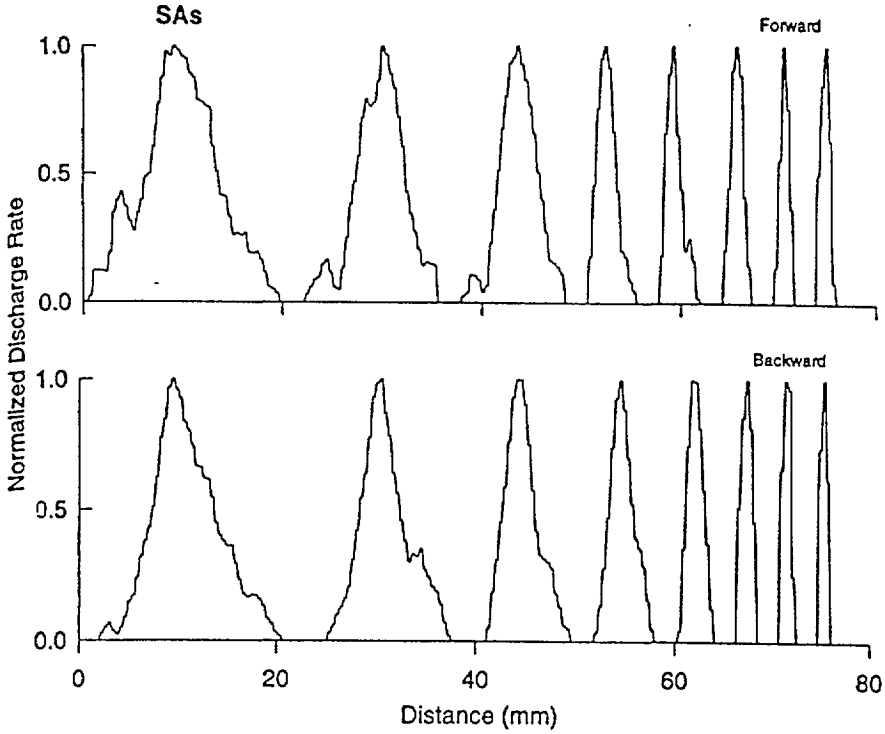

FIG. 14. Normalized spatial discharge rate profiles obtained from the mean SA response to each convexity of the wavy surface. Triangular response profile (above background) evoked by each convexity stroked in each direction was obtained from the SA responses in Fig. 12 (*top left* and *middle*) and normalized (see text).

vide a reliable estimate of the distribution of curvatures on the surface of an object.

Neural code for the shape of a cylinder

What is the peripheral neural code for a class of shapes that an object belongs to, in this case cylindrical bars, that will remain constant despite differences in size and the direction of stroking? In the following analysis, it is assumed that a central processor can normalize the spatial discharge rate profile evoked by each object (e.g., each convexity in the wavy surface) to some internal standard. For each triangular profile representing the mean response of the SA population to a given convexity stroked in a given direction, a horizontal line was drawn across its base at the points of minimal discharge rates. In the case of unequal minima, the horizontal line was passed through the higher value. Each discharge rate value above this line was normalized by first subtracting the base value and then dividing by the peak rate evoked by the convexity (Fig. 14). It is assumed that a central decoding mechanism can measure the change in slope from the base to the peak and from this peak to the base on the other side of the profile evoked by each convexity in the wavy surface. The data in Fig. 14 illustrate that each cylindrical convexity evoked the same tent-shaped triangular profile, the sides of which were approximately linear. Because each cylindrical convexity on the wavy surface had a constant curvature along its minor axis, we hypothesize that the peripheral neural code for a cylinder is the constancy of the slopes along the rising and falling phases of the spatial discharge rate profile evoked by the convexity in the SA population.

DISCUSSION

The responses of cutaneous mechanoreceptors to an object contacting the skin depend on the physical properties of the object, such as its compliance, texture, size, and shape, as well as how the object is applied to the skin, e.g., the compressional force, orientation, trajectory, and stroke velocity. In the present study it was found that the shape of the object as well as the stroke velocity and sometimes the direction of stroking modulated the responses of RA or SA mechanoreceptors.

The shape of a rigid object remains the same with changes in its orientation and translation as it is applied to the skin. This invariance is preserved when the object's shape is defined by the distribution of curvatures on its surface—in the present case a wavy pattern of cylindrical bars of different radii. Because the skin is compliant, it can change its initial shape to conform to the surface of the object in contact. Each convexity in the wavy surface, when stroked across a fiber's cutaneous receptive field on the fingerpad, produces a characteristic change in the curvature of the skin within the contact region. In response to a convexity followed by a concavity on the object's surface, the skin within the contact area changes from its normal convex shape to concave and then back to convex. These changes in skin curvature produce characteristic responses in the SA and RA fiber populations (Srinivasan and LaMotte 1991). The suitability of the discharge rates and their spatial distributions in each fiber population as candidate neural codes for shape will be discussed in the following sections.

Discharge rate

The discharge rates of SAs and RAs are the lowest when the stroke velocity is zero, that is, when the object is statically indented into the skin without stroking. When single cylindrical bars of different curvature were indented into the receptive fields of SAs and RAs on the monkey's fingerpad, RAs responded only during the indenting (ramp) phase but not during the plateau

phase of maintained displacement (LaMotte and Srinivasan 1993; Srinivasan and LaMotte 1991). Their discharge rates were not significantly modulated by differences in curvature ranging from 79 to 1,260 m^{-1} (2–32 $in.^{-1}$). Similarly, when sinusoidal step shapes were statically indented into the skin only SAs and not RAs responded to differences in step shape (Srinivasan and LaMotte 1987).

SAs responded to static indentations of cylindrical bars during both the ramp and plateau phases (LaMotte and Srinivasan 1993). Their discharge rates increased ~1.5 times during the ramp and about twofold during the plateau over a curvature range of ~79–315 m^{-1} (2–8 $in.^{-1}$). When cylindrical bars in the form of a wavy surface and having the same curvature range were stroked across the fingerpad in the present study, roughly the same doubling in discharge rates occurred in RAs as well as SAs within the range of stroke velocities tested (Fig. 6). For a given velocity of stroking, the discharge rates of both SA and RA mechanoreceptors increased as a function of increasing curvature of the convexities on the wavy surface. Similarly, when sinusoidal step shapes were stroked across the skin, discharge rates of both fiber types increased with increases in curvature (LaMotte and Srinivasan 1987a,b). Whereas the spatial profile of SA responses provided the best information on the overall shape of the step, the smallest differences in the "sharpness" of the steps were better signaled by differences in the discharge rates of RAs.

Although the discharge rates in single fibers or populations of fibers can potentially encode curvature, this code is confounded by the changes in discharge rate that occur with changes in stroke velocity, stroke direction, or compressional force. For example, as the velocity of stroking the fingerpad over a given convexity in the wavy surface increases, the burst rates of SAs and RAs increase and the number of impulses per burst as well as the number of impulses per millimeter decrease. Thus neither the impulse count per burst nor the rate of change of discharge with respect to temporal or spatial coordinates has an invariant relation with stroke velocity. Similarly, it has been shown that as the frequency of a sinusoidally vibrating probe or the temporal frequency of a grating stroked across the fingerpad increases, the impulse count per cycle (or bar) decreases (Goodwin et al. 1989).

If the stroke velocity changes considerably as the skin is moved back and forth over an object, the discharge rates of primary afferent fibers can signal differences in curvature only if independent information is available about the stroke velocity at any moment in time. Discernible features on an object's surface would sequentially activate different fibers with changes in the locus of the contact area during stroking. This is a likely source of information about the velocity of stroking during either active or passive touch. When the finger is actively moving over an object, kinesthetic cues provide additional information about stroke velocity. But even when information about stroke velocity is available, discharge rate is still influenced by other stimulus parameters such as stroke direction and contact force. Therefore differences in discharge rate can contribute to the sensory discriminations of shapes but do not provide a robust code for the identification of shape.

Spatial measures

The discharges of individual fibers, plotted as a function of spatial coordinates, can be interpreted as the spatially distributed responses of a population of fibers with identical response properties. This is clearly an idealization, because there are differences in response properties among fibers. Nevertheless, each fiber exhibited the same pattern of responses to the wavy surface and qualitatively similar responses to variations in curvature and stroke velocity. Thus both the SEPs and SRPs obtained from our sample of fibers provide reasonable representations of a population response in lieu of measuring the responses directly.

The spatial parameters derived from such SEPs, such as the widths of bursts of impulses and the pauses between bursts in the fiber population, provide neural codes for the sizes of the features on the object's surface contacting the skin (LaMotte and Srinivasan 1987a). This is consistent with the SEP being almost isomorphic to the two-dimensional outline of the portion of the shape in contact with the skin (Johnson and Hsaio 1992). For the wavy surface, the widths of bursts and pauses, representing cutaneous areas innervated by active and inactive afferent fibers, respectively encode the widths of the convexities and concavities on the surface of the object.

The widths of the bursts and pauses decreased significantly with increasing curvature in much the same way for each direction of stroking. Furthermore, the response width associated with any convexity or concavity changed little with changes in the velocity or direction of stroking. Similarly, the widths of impulse bursts in SEPs, obtained in response to sinusoidal step shapes stroked across the fingerpad, remained invariant with moderate changes in stroke velocity (LaMotte and Srinivasan 1987a). Thus, unlike the discharge rates within a population of fibers, which could be strongly influenced by changes in the direction and velocity of stroking, the spatial extent of fiber activity and inactivity provides a robust neural code for the size of a shape contacting the skin. However, this spatial extent represents at best a two-dimensional projection of a shape onto the skin but not the shape in three dimensions.

Spatial rate measures

With the use of a variety of embossed stimuli, Johnson and coworkers have shown that SEPs of SA and RA responses are isomorphic to the two-dimensional outline or form of the stimuli. However, the SRP, which represents a hypothetical population response in terms of a spatial distribution of discharge rate, is not isomorphic to the stimulus geometry in the third dimension of the stimuli perpendicular to the skin surface. This is evident in responses to the static indentations of gratings (Phillips and Johnson 1981), indentation and stroking of sinusoidal step shapes (LaMotte and Srinivasan 1987a,b; Srinivasan and LaMotte 1987), and the stroking of embossed letters and dots (Phillips et al. 1988, 1992). In SEPs, a higher density of dots at the leading edge indicates a higher discharge rate than at the trailing edge. Similar nonisomorphism in the SRP was observed for SA and RA responses to the stroking of the wavy surface where the cylindrical convexities gave rise to a triangular SRP.

When more than one convexity lay within the region of contact with the skin, a spatial measure of peak rate separation would be contained directly in the neuronal response at each instant of time. Otherwise such a spatial measure would have to be extracted indirectly by the brain from the product

of the time separating the occurrence of each peak and the stroke velocity.

Parameters related to the size of a shape or portion of a shape, although an important property of a particular shape, do not characterize the shape itself as belonging to a particular category such as a wavy surface, step, or cylindrical bar in the absence of additional information. A certain kind of shape can have different sizes, yet still be recognized as belonging to the same category. Similarly, the shape of a particular object may evoke different widths of activity in a population of fibers depending on the compressional force with which it is applied to the skin (Goodwin et al. 1991). It seems likely that the pattern of curvatures that characterizes a particular shape will be represented by the relative changes in the SRP in the relevant fiber populations. The SRP is smoother and less irregular for SAs than for RAs. That is, the spatial information about the shape of each curvature is better preserved in the discharges of SAs. How is this spatial representation decoded centrally? One possibility is that a central processing mechanism extracts the slopes at successive points along the SRP. Thus the distribution or sequence of such slopes along the SRP in the SA population would represent the shapes of each individual feature on a surface (e.g., a cylindrical convexity) as well as the overall shape of the pattern of features (aperiodic pattern of cylindrical features defining the wavy surface). With moderate changes in stroke velocity or force, although the magnitude of slopes might change, the pattern of slopes would not vary. In the case of the wavy surface, the constant curvature characterizing each cylindrical convexity is encoded by the constancy of the slopes on each side of the triangular spatial discharge rate profiles evoked in the SA fiber population parallel to the minor cylindrical axes.

The spatial profile of SA responses is not isomorphic with object shape, owing to the responsiveness of SAs to other parameters of stimulation besides the curvature of the object. One parameter is the rate of change in curvature, which is a function of the velocity of stroking as well as the amount of curvature. Another is the extent to which the skin can conform to a shape such as a concavity that lies between convexities. Although the concavities were in contact with the skin, the absence of sufficient force of contact will produce a pause in the discharge profile. Additional parameters that can directly influence the discharge rates of fibers include differences in fiber sensitivities as well as any biases in the directional sensitivities of individual SAs. A central processing mechanism for shape would then have to normalize the discharge rates, for example by comparisons with an internal standard, to take into account changes in rate due to the effects of these parameters.

We thank A. Klusch-Petersen, C. Lu, K. Dandekar, and T. O'Connor for technical assistance in data analysis.

This research was supported by National Institute of Neurological Disorders and Stroke Grant NS-15888 and Office of Naval Research contract N00014-91-J-1566.

Address for reprint requests: R. LaMotte, Dept. of Anesthesiology and Section of Neurobiology, 333 Cedar St., Yale University School of Medicine, New Haven, CT 06510.

Received 5 September 1995; accepted in final form 15 August 1996.

REFERENCES

DARIAN-SMITH, I. AND KENINS, P. Innervation density of mechanoreceptive fibres supplying glabrous skin of the monkey's index finger. *J. Physiol. Lond.* 309: 147–155, 1980.

GAUSS, C. F. Disquisitiones generales circa superficies curvas. *Commentat. Soc. Reg. Sci. Gottingen. Recentiores* 6: 99–146, 1827.

GOODWIN, A. W., BROWNING, A. S., AND WHEAT, H. E. Representation of curved surfaces in responses of mechanoreceptive afferent fibers innervating the monkey's fingerpad. *J. Neurosci.* 15: 798–810, 1995.

GOODWIN, A. W., JOHN, K. T., AND MARCEGLIA, A. H. Tactile discrimination of curvature by humans using only cutaneous information from the fingerpads. *Exp. Brain Res.* 86: 663–672, 1991.

GOODWIN, A. W., JOHN, K. T., SATHIAN, K., AND DARIAN-SMITH, I. Spatial and temporal factors determining afferent fiber responses to a grating moving sinusoidally over the monkey's fingerpad. *J. Neurosci.* 9: 1280–1293, 1989.

GOODWIN, A. W. AND WHEAT, H. E. Magnitude estimation of contact force when objects with different shapes are applied passively to the fingerpad. *Somatosens. Mot. Res.* 9: 339–344, 1992.

GORDON, I. E. AND MORISON, V. The haptic perception of curvature. *Percept. Psychophys.* 31: 446–450, 1982.

JOHANSSON, R. S., LANDSTROM, U., AND LUNDSTROM, R. Sensitivity to edges of mechanoreceptive afferent units innervating the glabrous skin of the human hand. *Brain Res.* 244: 27–32, 1982.

JOHANSSON, R. S. AND VALLBO, A. B. Tactile sensibility in the human hand: relative and absolute densities of four types of mechanoreceptive units in glabrous skin. *J. Physiol. Lond.* 286: 283–300, 1979.

JOHNSON, K. O. AND HSIAO, S. S. Neural mechanisms of tactual form and texture perception. *Annu. Rev. Neurosci.* 15: 227–250, 1992.

JOHNSON, K. O. AND LAMB, G. D. Neural mechanisms of spatial tactile discrimination: neural patterns evoked by Braille-like dot patterns in the monkey. *J. Physiol. Lond.* 310: 117–144, 1981.

JOHNSON, K. O. AND PHILLIPS, J. R. Tactile spatial resolution. I. Two-point discrimination, gap detection, grating resolution, and letter recognition. *J. Neurophysiol.* 46: 1177–1191, 1981.

LAMOTTE, R. H. AND SRINIVASAN, M. A. Tactile discrimination of shape: responses of slowly adapting mechanoreceptive afferents to a step stroked across the monkey fingerpad. *J. Neurosci.* 7: 1655–1671, 1987a.

LAMOTTE, R. H. AND SRINIVASAN, M. A. Tactile discrimination of shape: responses of rapidly adapting mechanoreceptive afferents to a step stroked across the monkey fingerpad. *J. Neurosci.* 7: 1672–1681, 1987b.

LAMOTTE, R. H. AND SRINIVASAN, M. A. Responses of cutaneous mechanoreceptors to the shape of objects applied to the primate fingerpad. *Acta Psychol.* 84: 41–51, 1993.

LAMOTTE, R. H., SRINIVASAN, M. A., LU, C., AND KLUSCH-PETERSEN, A. Cutaneous neural codes for shape. *Can. J. Physiol. Pharmacol.* 72: 498–505, 1994.

LAMOTTE, R. H., SRINIVASAN, M. A., LU, C., AND PETERSEN, A. K. Responses of cutaneous mechanoreceptors to two- and three-dimensional shapes stroked across the monkey fingerpad. *Soc. Neurosci. Abstr.* 19: 105, 1993.

LAMOTTE, R. H., WHITEHOUSE, G. M., ROBINSON, C. J., AND DAVIS, F. A tactile stimulator for controlled movements of textured surfaces across the skin. *J. Electrophysiol. Tech.* 10: 1–17, 1982.

PHILLIPS, J. R., JOHANSSON, R. S., AND JOHNSON, K. O. Responses of human mechanoreceptive afferents to embossed dot arrays scanned across fingerpad skin. *J. Neurosci.* 12: 827–839, 1992.

PHILLIPS, J. R. AND JOHNSON, K. O. Tactile spatial resolution. II. Neural representation of bars, edges, and gratings in monkey afferents. *J. Neurophysiol.* 46: 1192–1203, 1981.

PHILLIPS, J. R., JOHNSON, K. O., AND HSIAO, S. S. Spatial pattern representation and transformation in monkey somatosensory cortex. *Proc. Natl. Acad. Sci. USA* 85: 1317–1321, 1988.

SRINIVASAN, M. A. AND LAMOTTE, R. H. Tactile discrimination of shape: responses of slowly and rapidly adapting mechanoreceptive afferents to a step indented into the monkey fingerpad. *J. Neurosci.* 7: 1682–1697, 1987.

SRINIVASAN, M. A. AND LAMOTTE, R. H. Encoding of shape in the responses of cutaneous mechanoreceptors. In: *Information Processing in the Somatosensory System*, edited by O. Franzen and J. Westman. London: Macmillan, 1991, p. 59–69.

SRINIVASAN, M. A. AND LAMOTTE, R. H. Tactual discrimination of softness. *J. Neurophysiol.* 73: 88–101, 1995.

VIERCK, C. J. Comparisons of punctate, edge and surface stimulation of peripheral slowly adapting, cutaneous, afferent units of cats. *Brain Res.* 175: 155–159, 1979.